

EVALUATION FOR LOCAL SITE EFFECT OF SEDIMENTARY BASIN TAKING INTO ACCOUNT INCIDENT WAVE FIELD

Kiyotaka SATO¹, Sadanori HIGASHI², Shunji SASAKI³ and Kenzo TOKI⁴

¹Member of JSCE, M. Eng., Geotech. & Earthq. Eng. Dept, Central Research Institute of Electric Power Industry
(1646, Abiko, Abiko-shi, Chiba 270-1194)

²Dr. of Sci., Geotech. & Earthq. Eng. Dept, Central Research Institute of Electric Power Industry
(1646, Abiko, Abiko-shi, Chiba 270-1194)

³Dr. of Sci., Geotech. & Earthq. Eng. Dept, Central Research Institute of Electric Power Industry
(1646, Abiko, Abiko-shi, Chiba 270-1194)

⁴Fellow Member of JSCE, Dr. of Eng., Professor, Dept. of Civil Eng., Kyoto University,
(Yoshida Honmachi, Sakyou-ku, Kyoto city, Kyoto 606-0000)

Local site effects of two alluvial sedimentary basins at Kuno in Ashigara valley and at Takeyama in Miura peninsula were evaluated under strong motion array seismographs observation. The horizontal spectral ratios of the gravelly soil's sediments at Kuno were constant in the component along the S wave's principal axis corresponded to the focal radiation pattern. On the soft clay's sediments at Takeyama, the spectral ratios to a reference point at the outcrop of bedrock were constant by considering seismic incident angle. Thus the site effects computed by two-dimensional analytical method agree with the observed spectral ratios by considering the incident wave field related to the source and path effects.

Key Words: *local site effect, sedimentary basin, incident wave field, focal radiation pattern, path effect, irregularly layered media*

1. INTRODUCTION

Analytical methods on seismic wave field in irregularly layered media are directly related not only to evaluations of site effect based on geotechnical surveys and earthquake observation, but also to investigations of seismic path and source processes. Those total evaluations make it possible to synthesize strong motion¹⁾. Then it is important to interpret incident wave field based on seismic source and path effects, in order to evaluate quantitative local site effect during strong motion. If the quantitative site effect is evaluated on the basis of the incident wave field, it becomes possible to simulate input motion on the earthquake resistant design for various important structures.

We have strong-motion seismograph array observation sites at two sedimentary basins. One is a middle-sized gravelly diluvial and alluvial soil's basin which is located on Ashigara valley, Kuno, Japan, called AGK site²⁾ hereafter. The other is a small-sized soft clay's alluvial valley, which is located on Takeyama in Miura peninsula, called TKY site³⁾.

In both sites, several good seismic records have been observed. In this paper, it was studied about the relationship between the site effect and the incident wave field related to the source and path effects in each seismic event. Those results were interpreted by using those observed records and numerical analyses.

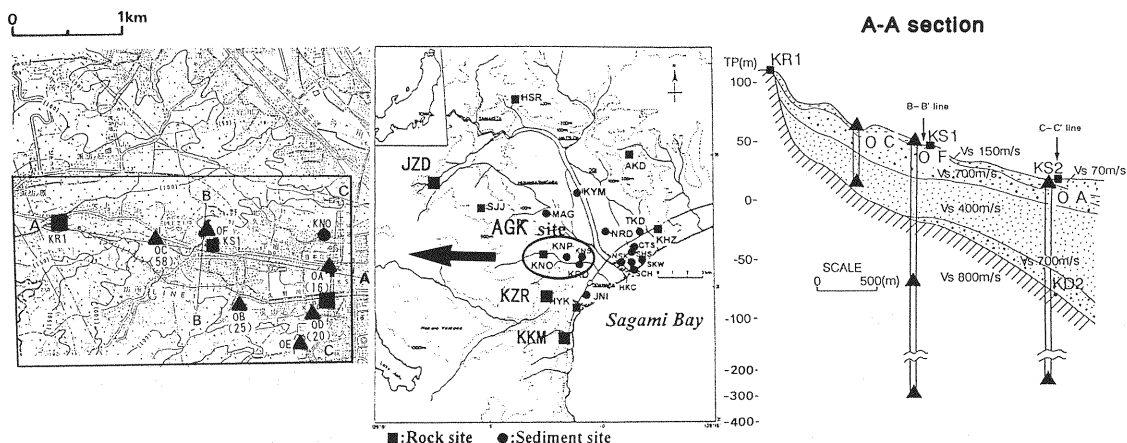


Fig.1 Magnified location map of array seismographs observation area at AGK site (▲ by EPCO, ● by CRIEPI, ■ by ERI) **Fig.2** Schematic cross-section ¹⁾ at OC, OF and OA

2. SEISMIC WAVE VELOCITY AT OBSERVATION SITES

(1) Gravelly soil's sediments in AGK site

Historical destructive earthquakes⁴⁾ have occurred repeatedly with return periods of about 70 years around Odawara area. So some seismologists⁵⁾ predict that a Western Kanagawa earthquake of magnitude 7.0 will occur in the near future. This is the reason why the Earthquake Research Institute (ERI) at the University of Tokyo and others as well as our research laboratory have already installed strong motion spatial and vertical array seismographs observation in this area. **Fig.1**⁶⁾ shows those observation points and the schematic cross-section along the east to west line's profile for the reflection survey, which are giving a two or three dimensional image of geological structure in the observation site.

AGK site and its vicinity have been geophysically explored to investigate velocity structure and physical properties of the subsurface structure. Logging provides valuable data for understanding geotechnical properties of soil deposits at downholes of AGK site. P- and S-wave velocity logging has been carried out in five downholes, called OA, OC, OD, OE and OF, hereafter ranging from the depth of 20m to 330m, where suspension method in the logging and the vertical seismic profiling (VSP) survey⁷⁾ were applied. The P- and S-wave velocities are

indispensable to seismic response analysis for the irregularly layered media. Furthermore electrical normal logging and density logging were also conducted in the downholes site.

In the other observation points installed by ERI, there are three downholes ranging from a depth of 20 to 100m called KS1, KS2 and KR1. The downhole method of seismic survey was applied in the downholes. From these results, it was clarified that S-wave velocity is about 65~170m/sec for alluvial humus soil and silt, 340~430m/sec for loam, 620~750m/sec for pumice flow (gravel), 400~500m/sec for pumice flow (sand) and 700~1200m/sec for pyroclastic material, respectively. P-wave velocity of each stratum also reveals various values ranging from 400 to 2400 m/sec and the values of density variable between 1.4 and 2.5 g/cm³. **Fig.2** shows schematic cross section of OC, OF and OA.

(2) Soft clay's sedimentary basin in TKY site

TKY site is located on the middle part at the east shore of Miura peninsula and facing on the east of Sagami bay. Miura peninsula is based on Hayama group of old Tertiary. Miura and Sagami groups are distributed on upper layer of the Hayama group. Gravel and loam layers are distributed on the terrace formation. Alluvial layers are distributed over the lower land in this district. On the basis of geological surveys³⁾ in TKY site, it was confirmed that the rock of Miura group is outcrop at the west side and Hayama

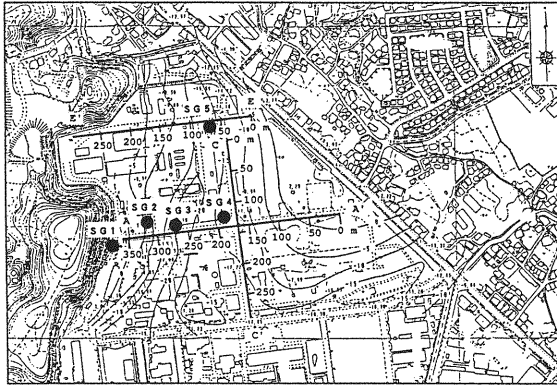


Fig.3 Location of array seismographs and three bold lines measured by shallow reflection survey at TKY site (Contour lines mean the depth of rock)

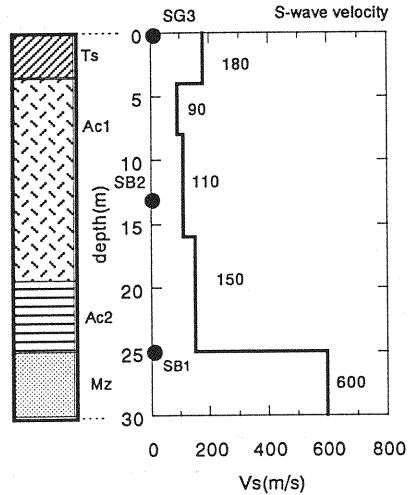


Fig.4 Geotechnical profile at TKY site

Table1 Recorded earthquakes' property at AGK site

EQ No.	Name of Earthquake	Date	Origin time	Latitude	Longitude	Depth (km)	Magnitude Mj	Epicentral distance from AGK (km)	Epicentral distance from TKY (km)
1	Suruga bay	1995/4/18	20:26	35° 03'	138° 35'	24	4.5	57.0	—
2	Sagami bay	1995/7/3	8:53	35° 09'	139° 34'	122	5.2	40.0	8.2
3a	E. Yamanashi	1996/3/6	23:12	35° 30'	138° 54'	16	4.3	34.5	—
3b	E. Yamanashi	1996/3/6	23:35	35° 30'	138° 54'	17	5.3	34.5	—
4	E. Off. Chiba	1996/9/11	11:37	35° 38'	141° 12'	53	6.2	190.4	153.9
5a	E. Yamanashi	1996/10/25	12:25	35° 27'	139° 00'	23	4.5	24.6	61.7
5b	E. Yamanashi	1996/10/25	21:06	35° 28'	138° 59'	18	4.1	26.9	—
6	E. Off. Izu Penin.	1997/3/4	12:51	34° 10'	139° 10'	2	5.7	35.2	49.5
7	S. Ibaraki	1997/3/23	20:36	35° 58'	140° 06'	72	5.0	—	103.6
8	W. Kanagawa	1997/11/4	10:31	35° 12'	139° 06'	20	3.9	9.1	—

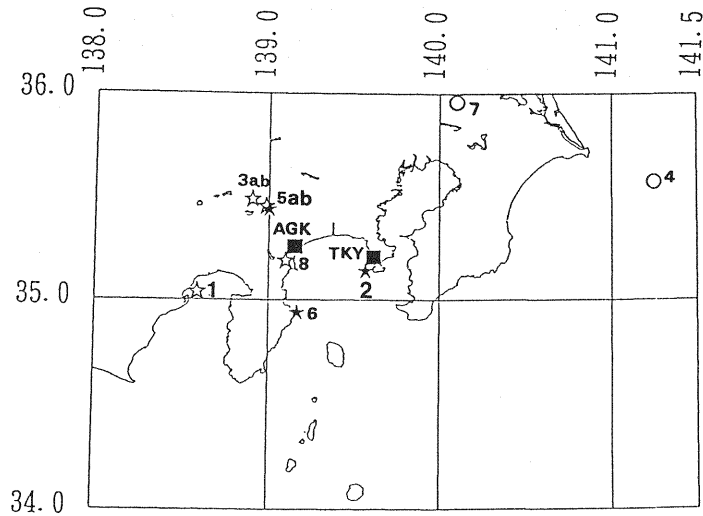


Fig.5 Analyzed seismic epicenter and observation locations (☆:AGK record, ○:TKY record, ★:both sites record, ■:observation site)

group is distributed on the east side. It was also recognized that this is a typical small sized sedimentary basin along the west to the east.

As seen in Fig.3, P-wave seismic reflection surveys in shallow layer were carried out at measured lines of A-A', C-C', and E-E', respectively. 3-dimensional soil profile was analyzed at the three sections. From these surveys, it is clarified that this site is a sedimentary basin, which is 300m wide and 25m deep. P-wave velocities of basement soft rock were 1.9km/s except only weathering rock.

Vertical distribution along the depth of SG3 for P- and S-waves velocities were obtained from PS logging as seen in Fig.4. P-wave velocities were ranging from 400 to 1200 m/s in alluvial layer and 1900 m/s in basement layer. S-wave velocities were ranging from 90 to 180 m/s in first clay of Ac₁ layer, 150 to 180 m/s in second clay of Ac₂ layer underlain the bottom of alluvial sedimentary basin, and 600 m/s in soft rock of Miura group's Zushi layer.

3. FOCAL RADIATION PATTERN AND SEISMIC PATH EFFECT FOR THE RECORDED SEISMIC EVENTS

Earthquake events in 3 source regions were recorded at the same time at both observation sites as seen in Table 1 and Fig.5. In this section, those common seismic records and the others in each site were investigated about the focal radiation pattern and seismic path effect.

(1) AGK site

Main earthquake events in 5 source regions were recorded from April in 1995 to November in 1997. These events are Western Kanagawa earthquake (EQ.8) at a near-field epicentral distance of 9.1km and the other earthquakes, East Yamanashi (EQ.3a,3b,5a,5b), East off Izu peninsula (EQ.6), Suruga bay (EQ.1) and Sagami bay (EQ.2) those which occurred in the region from about 20 to 60 km epicentral distance at surrounding locations of AGK site. The magnitudes of those events were small and middle sized earthquakes scaled from 3.9 to 5.7 and most of recorded events were shallow earthquakes at the focal depth less than about 70km except Sagami bay earthquake which had a depth of 122km. Even if large scaled earthquakes, such as E. Yamanashi(EQ.3b) and E. off Izu peninsula(EQ.6) earthquakes, the length of those faults obtained from

the empirical equation estimated by Matsuda⁹⁾ was much smaller than the epicentral distance. So those events were identified as a point source with respect to AGK site.

First, the focal S-wave radiation patterns of those earthquakes were induced by moment tensor solution M_{pq} as a point source⁹⁾. The source parameters, such as a strike angle ϕ , dip angle δ and slip angle λ in the source fault estimated by the National Institute for Earth Science and Disaster Prevention(NIED) were obtained as seen in Table 2. The S-wave focal radiation patterns given by moment tensor solution in those source parameters were the following equations for SH and SV waves as a dimensionless form. It is a Green function, which induced the far-field displacement for a point source in a homogeneous medium.

$$F_{SV} = V_p \gamma_q M_{pq} \\ = \sin \theta \cos \theta (\cos 2\phi M_{xx} + \sin 2\phi M_{xy} + \sin 2\phi M_{yy} - M_{zz}) \\ + \cos 2\theta (\cos \phi M_{xz} + \sin \phi M_{yz}) \quad (1)$$

$$F_{SH} = H_p \gamma_q M_{pq} \\ = \sin \theta [\sin \phi \cos \phi (M_{xx} - M_{yy}) + \cos 2\phi M_{xy}] + \cos \theta \\ + \cos 2\theta (\cos \phi M_{yx} - \sin \phi M_{xz}) \quad (2)$$

where M_{pq} is moment tensor, $V_p \gamma_q$ is a unit vector in the SV direction and $H_p \gamma_q$ is a unit vector in the SH direction. The S wave radiation patterns for SH and SV waves like as seen in Fig.6 were obtained on every 10 degrees at the azimuth and the take-off angles by using the above functions. Then the vectors were indicated as an equal area projection of the lower hemisphere of the focal sphere in Fig.7. The amplitude of vector is represented as ten steps from 0.1 to 1.0 every 0.1. The radiation patterns for every event were computed by the resolution of above moment tensor. Table 3 shows the azimuth and take-off angles to the OA observation point for each seismic source, based on the earth's crust structure¹⁰⁾ evaluated by artificial explosive seismic survey in Izu district as seen in Table 4. In the case of E. Off Izu peninsula earthquake, the SH wave's radiation pattern is predominantly larger than the SV wave's one as seen in Fig.8. In Fig.9, the S wave principal shocks are traced for the velocity seismograms at the surface of the sedimentary basin on OC, OF, and OA filtered by the Chebishev's band pass filter(BPF) at the range from 0.4 to 1.0Hz. In Fig.9, S wave's first motion of the velocity seismograms is

Table 2 List of CMT solution for the analyzed seismic source(by NIED:<http://www.bosai.go.jp/jindex.html>)

EQ.No	strike ϕ s(deg)	dip δ (deg)	slip λ (deg)	Magnitude Mj	depth h(km)
1	162.0	56.7	166	4.5	24
2	252.0	83.8	114	5.2	122
3b	24.3	50.0	102	5.3	20
4	132.0	63	-50	5.0	53
5a	207.0	35.0	90	4.5	23
6	69.8	58.2	-154	5.7	2
7	118.8	59.5	64.3	5.0	72
8	232.0	80.0	158	3.9	15

calaloged by NIED

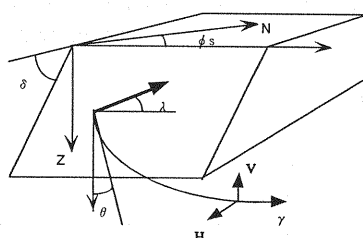


Fig.6 Diagrams for source parameters

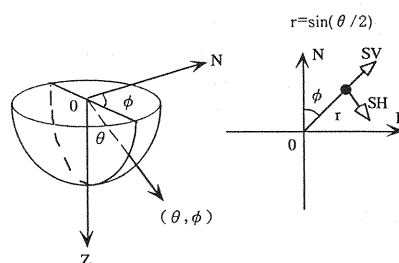


Fig.7 Diagram for an equalarea projection of the lower hemisphere of the focal sphere

Table 3 Estimated azimuth and take-off angles for AGK site

EQ.No.	unit(degree)	
	azimuth Φ	take-off θ
1	66	60
2	290	161
3b	139	118
5a	146	120
6	356	58
8	32	148

Table 4 Earth's crust structure in Izu district

Layer No.	Thickness (km)	Vp (km/s)	Vs (km/s)	ρ (t/m ³)
1	1.0	3.0	1.2	2.2
2	3.0	5.0	2.7	2.8
3	15.0	5.9	3.7	2.8
4	11.0	6.8	3.9	3.0
5	∞	7.7	4.4	3.3

apparently predominant in EW component much more than it in NS component. It is coincided with the focal radiation pattern. In the case of W. Kanagawa(EQ.8) and E. Yamanashi earthquakes (EQ.5a), the SV wave's radiation pattern is predominantly larger than the SH wave's one. The azimuth angle to OA from southwest direction in W. Kanagawa earthquake was 32 degree and the azimuth angle from northwest in E. Yamanashi earthquake was 146 degree. So the S wave's first motions were predominant along both NS and EW components. But in E.Yamanashi earthquake(EQ.3b), the S wave's principal axis was found to be inclined along EWdirection of the sedimentary valley by the effect of the path process in the geological structure of Ashigara valley¹¹⁾. On the other hand, the SH wave's radiation patterns

were so larger than the SV wave's ones in Suruga bay and Sagami bay earthquakes(EQ.1&2). Then the first S waves were predominantly larger in NS component than those in EW component. Those results of the seismograms mean that the S wave's principal axis is in response to the focal radiation pattern.

At the downhole seismograph observation sites such as OA, OC, OD, OE, and OF, the spectral ratios between the surface and the basement layers were analyzed for the S wave's principal shock in horizontal components.

Analyzed seismic records were divided into the groups of NS and EW predominant earthquakes concerning the S wave's principal axis due to the focal radiation. The spectral ratios were compared concerning two groups of earthquakes.

Suruga bay and Sagami bay earthquakes (EQ.1 & 2) are the NS predominant group for the S wave's principal axis. E. Yamanashi(EQ.3b & 5a) and E. Izu peninsula(EQ.6) earthquakes are EW predominant group for the S wave's principal axis. Only a W. Kanagawa earthquake belongs to both groups because the S wave's principal axis is predominant along both NS and EW components.

As seen in a result of **Fig.10(a)**, the spectral ratios appeared as constant characteristics in a low frequency region less than 2.5Hz in the EW component along the S wave's principal axis in the EW predominant group. On the other hand as seen in **Fig.10(b)**, the spectral ratios, of which peaks' amplitude were clearly fluctuated around 1Hz for every earthquake, apparently appeared as variable characteristics in EW component along the orthogonal direction to the S wave's principal axis in the NS predominant group. Although, the spectral ratio in the component normal to the S wave's principal axis also represent the site amplification characteristics on OA in a feature of whole spectral shape.

According to these results, it was clarified that the spectral ratios' property was constant in the low frequency region for the principal axis corresponded both to the focal radiation pattern and to path effect. So the site amplification on AGK is affected by both of the sedimentary basin and the incident wave field related to the source and path effects.

(2) TKY site

Sagami bay(EQ.1), E. Yamanashi pref.(EQ.5a) and E. Off Izu peninsula(EQ.6) earthquakes were also observed at the same time on array seismographs observation system in TKY site. These events are about 50 to 60km epicentral distances except a Sagami bay earthquake which is located on 122km deep in the near field. On the other hand, South Ibaraki pref.(EQ.7) earthquake scaled $M_j=5.0$ and E. Off Chiba pref.(EQ.4) earthquake scaled $M_j=6.2$ are located in 104 and 154 km epicentral distances. The focal radiation patterns as a point source and the site effects for those earthquakes were investigated as well as those at AGK site.

With respect to E. Off Izu peninsula earthquake, the S wave radiation patterns for SH- and SV-waves were obtained as an equal area projection of the lower hemisphere of the focal sphere like as seen in **Fig.11**. The azimuth and take-off angles to TKY

site were obtained by using the earth's crust structure in Izu district. Those were plotted on the same figures. On the focal radiation patterns, the SH wave's radiation pattern was predominant larger than the SV wave's one as well as those results at AGK.

The velocity seismograms on rock and sediments were represented in **Fig.12**. As a result of the seismogram at SG1 on rock, the S wave's principal axis was predominant in NS component larger than it in EW component according to the focal radiation pattern, as similar as it on AGK. However as to the velocity seismograms on the sediments at TKY, the S waves were amplified in EW component on SG3, SG4 and SG5 as same as amplified in NS component. The principal axis was evaluated by the polarization analysis method⁹⁾ for 4 sec duration of the S wave's principal shock at a band pass filter's range from 1.0 to 2.5 Hz. Those were represented in the horizontal plane at each point as seen in **Fig.13**. The principal axis was inclined a little to EW direction at SG2 at the edge of sedimentary basin on a steep dipping base layer, although it was according to the focal radiation pattern in a low frequency region. The S wave's principal axis on SG3 is inclined a little along NS direction at the central part of the basin. The other S wave's principal axis on SG4 at the edge of the sedimentary basin on a gentle dipping base layer and on SG5 in a little narrow basin at the north area of TKY site were inclined to EW section as well as it on SG2.

Similar characteristics of the S wave's principal axis were founded for E. off Chiba pref., Sagami bay and S. Ibaraki pref. earthquakes. As seen in **Fig.14**, the strongest velocity seismograms were recorded during Sagami bay earthquake. Its S waves were amplified larger at SG3, SG4 and SG5 in a central part of the sedimentary basin. The secondary surface waves are induced by the edge effect of the basin as seen in **Fig.15**. Those waves are traced at a later part of the S wave's principal shock in NS component perpendicular to the sedimentary basin's profile. These results represent that the site effect is mostly effected by a lateral irregularity of the basin. Because this site is high contrast ground with impedance ratio factor less than 0.2 between the alluvial clay and the sandstone. Therefore the local site effect is influenced much more remarkably by the underground structure at TKY than by the incident wave field. Furthermore it was recognized that the vertical motion was amplified at SG2 on a steep

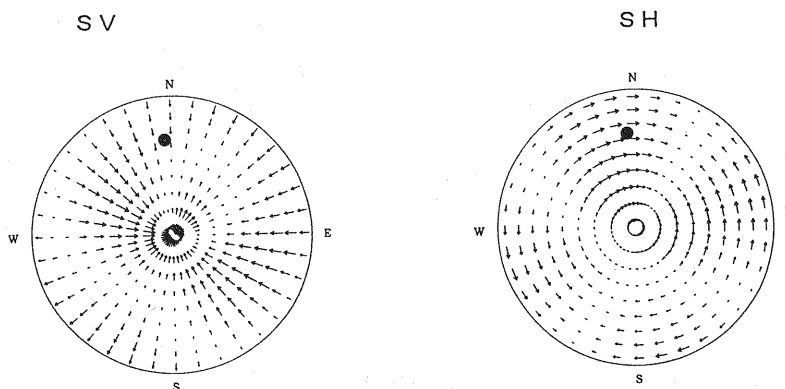


Fig.8 Focal radiation pattern of the lower hemisphere of the focal sphere for E. off Izu peninsula EQ.6
(Left: SV wave, Right: SH wave, ●:OA point)

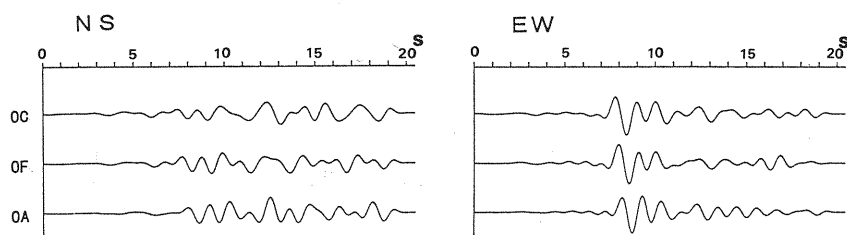


Fig.9 Horizontal BPF velocity seismograms on the AGK sedimentary basin (BPF range: 0.4 - 1.0Hz , EQ.6: E.off Izu penin.)

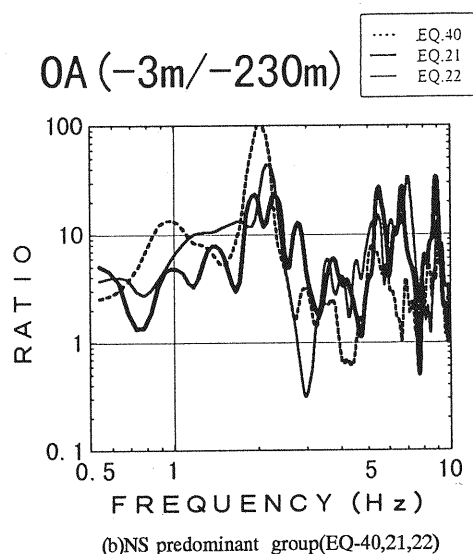
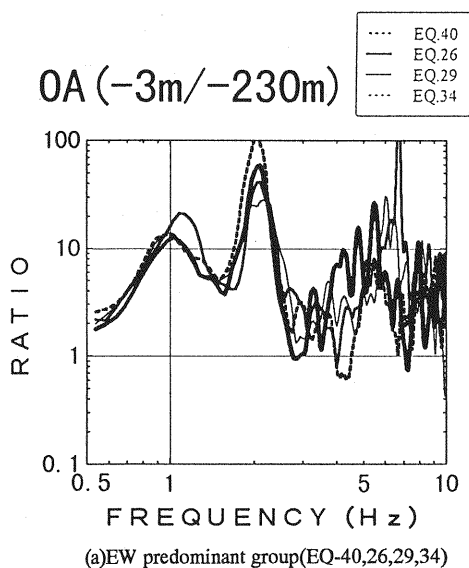


Fig.10 Spectral ratios between the surface and bottom at downhole array seismographs in EW component

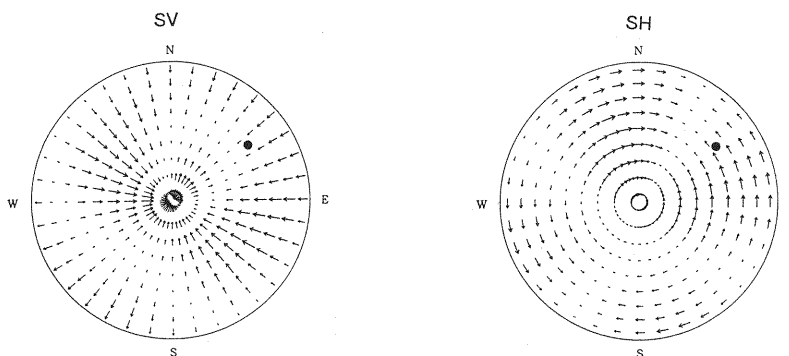


Fig.11 Focal radiation pattern of the lower hemisphere of the focal sphere for E. off Izu peninsula EQ.6(Left: SV wave, Right: SH wave, ●: TKY point)

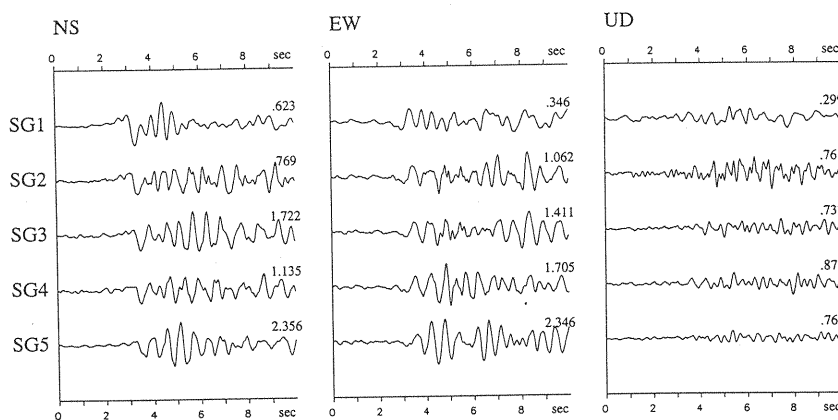


Fig.12 Velocity seismograms on the TKY sedimentary basin(EQ.6: E. off Izu peninsula)

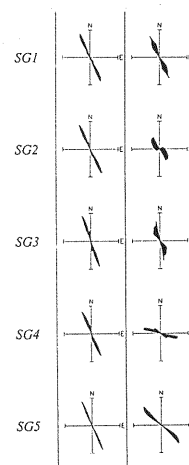


Fig.13 principal axis for horizontal motion (T=2.0-6.0sec, Left:BPF0.4-1.0Hz, Right:BPF1.0-2.5Hz)

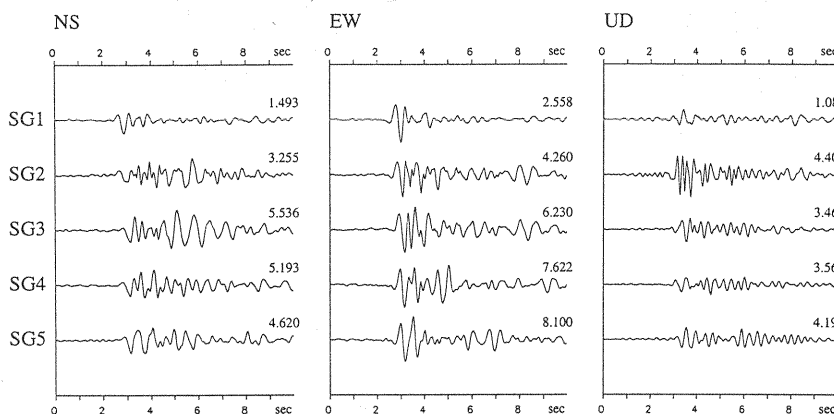


Fig.14 Velocity seismograms on the TKY sedimentary basin (EQ.2: Sagami bay)

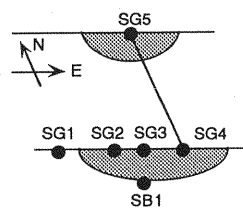


Fig.15 Schematic observation points at TKY site

dipping base layer larger than it on the other gentle dipping.

4. MODELING OF IRREGULARLY LAYERED MEDIA

(1) AGK site

As seen in the left hand of **Fig.16**, the models of deep sediments and basement rock over a depth of 300m were made by identified geotechnical parameters due to spectral inverse analysis method¹²⁾ in EW component on the reference of investigated PS logging's results, VSP survey²⁾, and seismic reflection survey²⁾. Two-dimensional (2D) response analysis was conducted on this model. The model is consisted of sediment layers for Hakone volcanic gravel(Hp(g)) or sand (Hp(s))and of basement rock for old Pleistocene layer(Os). Alluvial layer was excepted from the model. The geotechnical parameters such as seismic velocity and damping factor were given each layer as seen in **Table 5**.

Two-dimensional response analyses^{13), 14)} due to both anti-plane SH- and in-plane SV- wave incidence of the model by using Aki-Larner(AL) method were conducted. At that time, we considered the incident wave field written in chapter 3. One-dimensional (1D) analyses at the downhole array seismographs observation points were compared with the two-dimensional (2D) analyses. The one-dimensional layered models were made at each point of OF and OA. Those geotechnical parameters were the same as the 2D model. Ricker wave¹⁴⁾ with the natural frequency of 1.0 Hz was used as an incident wave. The computed spectral ratios were compared with the observed ones between the surface and basement seismograms as already shown in the previous chapter.

As seen in **Fig.17(a)**, the spectral ratios computed by 2D analysis due to SH wave incidence were compared with those of the NS predominant group for the S wave's principal axis, which were Suruga bay (EQ.1), Sagami bay (EQ.2) and W.Kanagawa earthquakes (EQ.8). The anti-plane direction of the 2D model is along NS component. So the computed spectral ratios on OC, OF and OA in AGK almost coincided with the observed ones regarding frequency characteristics in both 1D and 2D analyses. The amplification factor computed by 2D analysis agrees with the observed one in the low frequency range around 0.8Hz on OF and around the spectral peak

frequency of 1.5Hz on OA, better than those computed by 1D analysis.

On the other hand, as seen in **Fig.17(b)**, the spectral ratios computed by 2D analysis due to SV- incidence were similarly compared with those of the EW component's seismic group for the S wave's principal axis, which was E.Yamanashi (EQ.3b,5a), E. off Izu peninsula (EQ.6) and W.Kanagawa earthquakes (EQ.8). As a result, the site effects on OC, OF and OA similarly agree with the observed ones as to frequency characteristics. The constant spectral ratios had a little different characteristic in two horizontal components. The difference could be interpreted by 2D analysis for around 1.0 Hz on OF and 1.5 Hz on OA. Thus, 2D analysis due to SH- and SV- wave incidence are useful to compute irregular layered media considering incident wave fields during strong motion.

(2) TKY site

2D irregularly layered models were made as for the two sections of EW direction on the basis of the shallow reflection surveys and PS loggings as seen in **Fig.18**. Those geotechnical parameters were given for sedimentary layer and bedrock. The models are shapes of sedimentary-filled valleys, which are non-symmetrical 300m long and symmetrical 240m long models with 25m deep sediments at both central parts of SG3 and SG5, respectively. 2D analyses were conducted by using AL method^{13), 14)} as well as AGK site.

S-wave velocities are 133m/s in the alluvial layer and 600m/s in the soft bedrock. SG1 is set on the outcrop of bedrock at the west of the basin edge. S wave velocity measured by elastic wave's velocity exploration was 900m/s at the surface of the outcrop. This value represents seismic velocity of bedrock in TKY site. Ricker wave's natural frequency as the incident wave was 1.3Hz corresponded to 1-D ground model of the 25m thick sedimentary layer.

The S wave's spectral ratios of the surface seismograph's point to two reference points of SG1 at the outcrop and of SB1 at the bottom of the downhole were compared respectively with the computed spectral ratios due to 2D analyses. The recorded earthquakes were divided into two groups. One is the group of Sagami bay, E. off Izu peninsula and E. Yamanshi earthquakes located at the west to TKY. The other is the group of S. Ibaraki and E. Off Chiba earthquakes located at the east side to

Table 5 Geotechnical parameters in 1-D and 2-D model

Geology	Age	Vs(km/s)	Vp(km/s)	Q	ρ (t/m ³)
Hp(g)	late Pleistocene	0.7	2.0	50	1.9
Hp(s)	late Pleistocene	0.4	2.0	50	1.8
Hp(g)	late Pleistocene	0.75	2.5	50	2.0
Os2	middle Pleistocene	1.2	3.0	50	2.2

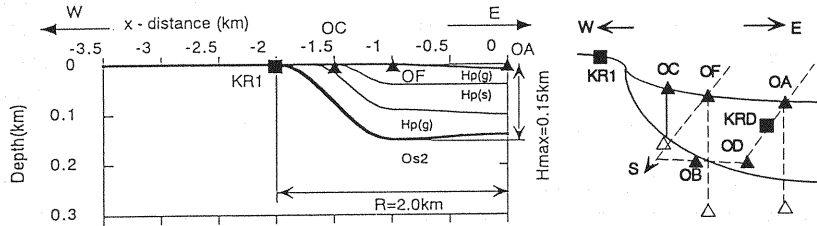


Fig.16 Geotechnical 2-D model and schematic observation points at AGK site

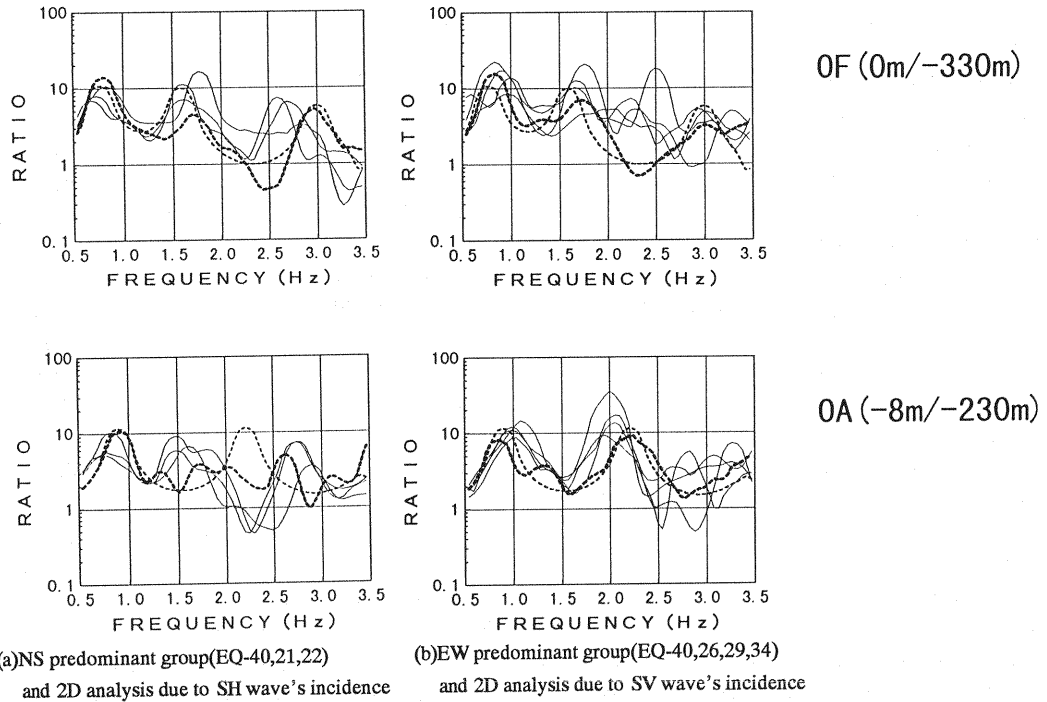


Fig.17 Comparison of analyzed and observed spectral ratios at OF and OA sites

[Thin line: Observed, Bold broken line: 2D analysis, Thin broken line: 1D analysis]

Table 6 Estimated azimuth and take-off angles for TKY site
unit(degree)

EQ.No.	SG1		
	azimuth Φ	take-off θ_o	incident θ_i
2	212	6	1.6
4	72	78	15.5
5a	295	85	17.9
6	234	58	22
7	28	59	13.6

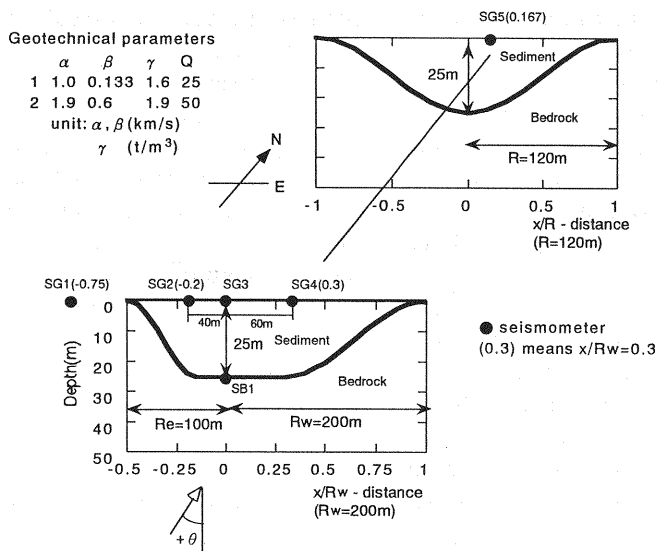


Fig.18 Geotechnical 2-D model and observation points at two EW sections on TKY site

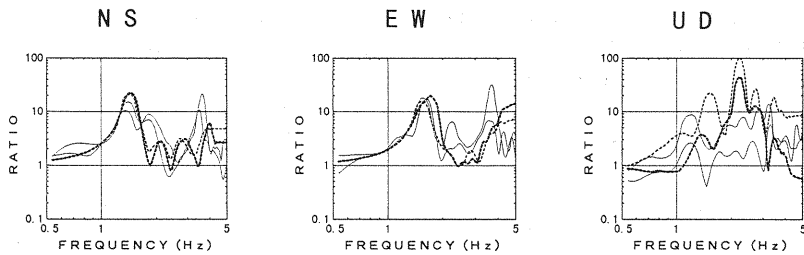


Fig.19 Comparison of spectral ratios between the surface and bottom of downhole array seismographs
 (Thin line: EQ.4 & 7, Broken line: 2D due to vertical incidence, Bold line: 2D due to 15 degrees oblique incidence)

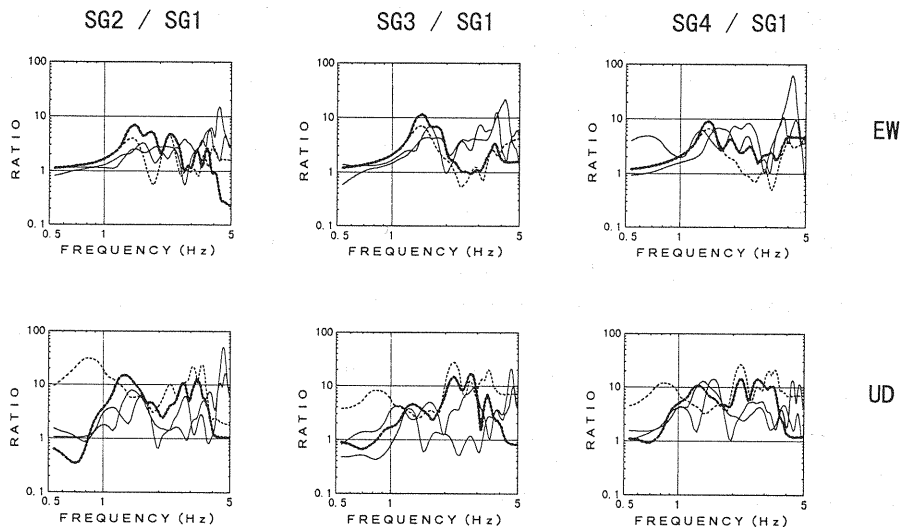


Fig.20 Spectral ratios of SG2, SG3 and SG4 to a reference point of SG1 on the outcrop of bedrock
 (Thin line: EQ.4 & 7, Broken line: 2D due to vertical incidence, Bold line: 2D due to 15 degrees oblique incidence)

TKY. Incident angles for all of recorded earthquakes were estimated by ray theory in the earth's crust structure to consider the phase difference of incident wave field. At this time, the earth's crust structure¹⁰⁾ estimated by explosive seismic survey in Izu district was used except the S wave velocity of 900m/s in soft bedrock at TKY site. 2D analyses due to both of anti-plane SH- and in-plane SV- wave incidence were computed.

As seen in **Table 6**, the seismic incident angles were indicated about 15 degree for the east earthquake group and the region less than 20 degree for the west earthquake group. Then 2D analyses due to both of the 15 degree oblique incidence from the east side and the 20 degree oblique incidence from the west side were computed as well as 2D analysis due to the vertical incidence.

As shown in **Fig.19**, the computed horizontal spectral ratios to a reference point of SB1 at the downhole's bottom agree with the observed ones and are not related to the seismic groups. But the computed vertical spectral ratios due to vertical and oblique SV- wave incidence don't agree with the observed ones well, since the observed ones are variable for each earthquake.

Concerning another spectral ratios to a reference point of SG1, the computed ones due to oblique SV-wave incidence agree with the observed ones in both components of horizontal EW and vertical UD much better than the computed ones due to vertical SV-wave incidence as seen in **Fig.20**. In the case of 2D analysis due to 15 degree oblique SV- wave incidence from the east side, the computed spectral ratios to a reference point of SG1 were different from the computed ones due to the vertical SV- wave incidence. Those differences were found apparently in the computed spectral ratios due to 20 degree oblique SV-wave incidence from the west side.

Therefore the local site effect is constant in TKY site and not related to the incident wave field because of the high impedance ratio between the sedimentary and the bedrock layers. But when site effects are evaluated by using spectral ratios to a reference point at the outcrop of bedrock, it is needed to consider the effect of the sedimentary basin on the seismograms at the reference point in accordance with the incident wave's incoming direction and incident angle. Because it is confirmed that the spectral ratios to a reference point at the outcrop of bedrock were different by related to the source locations. Thus if

2-D response analysis is conducted by taking into account the incident angle, it is possible to evaluate both of horizontal and vertical site effects on a sedimentary basin with high impedance ratio to bedrock. This conclusion represents it is needed to consider the incident wave field such as the incident angle and the incoming direction, because the spectral ratios to both references of outcrop's rock and downhole's bottom are different even if the spatial separation is less than 100 m distance like as TKY site.

5. CONCLUSIONS

On the basis of the gravelly soil's sedimentary basin in AGK site, the following was concluded.

(1) All of recorded earthquakes were analyzed as a point source. As a result, the predominant direction of the S-wave in sedimentary layer were corresponded to the focal radiation pattern.

(2) Based on the results concerning spectral ratios between the surface and bottom seismograms of the principal S-wave, apparently the site amplification characteristics was constant in the low frequency region less than 2.5 Hz in the component along S-wave's principal axis corresponded to the focal radiation pattern and seismic path effect. Thus the local site effect is influenced by both factors of the local underground structure and the incident wave field related to the source and path effects.

On the basis of the soft clay's sedimentary basin in TKY, the following was concluded.

(3) The spectral ratios to a reference point of downhole's bedrock were constant and not related to the source and path effects. But it was realized that the spectral ratios to a reference point at the outcrop of bedrock were different in accordance with the incident wave field even if the spatial separation is less than 100 m.

(4) It is possible for 2-D response analysis due to in-plane SV-wave incidence to evaluate the site amplifications in both components of horizontal and vertical on a sedimentary basin with high impedance ratio to bedrock. This conclusion represents the necessity to consider the incident wave field such as the incident angle and the incoming direction, when the spectral ratios to a reference at the outcrop of bedrock were used.

After all, the following was concluded

(5) Local site effects of small and middle sized sedimentary basins, is variable and related to the incident wave field. Thus it is useful for 2D response analyses due to SH- and SV-wave incidence taking into account the incident wave field to evaluate site amplification characteristics.

ACKNOWLEDGEMENT: This research was conducted as a common project of all electric power industry which are 9 electric power company and Japan nuclear power cooperation. Some of seismic records were provided by Dr. Kazuyoshi Kudo, who belongs to Earthquake Research Institute, University of Tokyo. We deeply appreciate all of them.

REFERENCES

- 1) Kawase, H.: Amplification of seismic waves by sedimentary layers and its simulation; Zisin Vol.46, No.2, pp171-190,1993 (in Japanese).
- 2) Sato, K., Higashi, S., Shiba, Y., Yajima, H. and Sasaki, S. : Site amplification and incident wave field at Kuno in Odawara city during 1996 East Yamanashi earthquake, CRIEPI Report U98061,1998 (in Japanese).
- 3) Sato, K. , Higashi, S., Shiba Y. and Abe, S. : Seismic amplification of irregular subsurface layer — Various geological survey and modeling for subsurface layer and seismic amplification characteristics based on earthquake observation — , CRIEPI Report U95061, 1996 (in Japanese).
- 4) Ishibashi, K. : Possibility of a large earthquake near Odawara, central Japan, preceding the Tokai earthquake, Earthq. Predic. Res., vol.3, pp319~344, 1985.
- 5) Ishibashi, K. : East Kanagawa earthquake and earthquake prediction I and II, the Science, vol.58, pp.537~547, 771~780, 1988 (in Japanese).
- 6) IASPEI/IAEE Joint WG and Japanese National WG: Proceedings of the International Symposium on the Effect of Surface Geology on Seismic Motion, ESG 1992 Vol II , March 1992.
- 7) Higashi, S. , Sato, K., Yajima, H., Sasaki, S. and Ishikawa, H. : Underground structure of Kuno-site on the basis of reflection seismic survey, Academic association of earth and planet, p142, B42-P12, 1997 (in Japanese).
- 8) Matsuda, T. : Magnitude and return period of earthquake occurred from active fault, vol. 128, pp.269-283, 1974 (in Japanese).
- 9) Kennet, B.L.N. : Radiation from a Moment-Tensor Source, Seismological Algorithms, pp.427-441, 1988.
- 10) Yoshii, T., Asano, S., Kubota, S., Sasaki, Y., Okada, H., Masuda, T., Murakami, H., Suzuki, S., Moriya, T., Nishide, N. and Inatani, H. : Detailed Crust Structure in the Izu Peninsula as Revealed by Explosion Seismic Experiments, J. Phys. Earth, 34, Suppl., 1986.
- 11) Higashi, S., Sato, K., Yajima, H., Sasaki, S. and Ishikawa, H. ; Analysis of incident wave field on Kuno site, The 10th JEES, October 1998.
- 12) Ishida, K., Sawada, Y., Sato, K. and Yajima, H. : Concerning a damping of soil - Estimation of Q-value by applying spectral inverse method - The proceeding of the seismological society of Japan, Autumn meeting 1984
- 13) Aki, K. and Larner, K. : Surface motion of a layered medium having an irregular interface due to incident plane SH waves", Journal of Geophysical Research, Vol.75, No.5, February 1970.
- 14) Ohori, M. : Seismic response analysis of sedimentary basin by using two-dimensional AL method, Journal of Zishin, vol165, 1990.

(Received July 31, 1998)